ORIENTALE MULTI-RINGED BASIN INTERIOR AND IMPLICATIONS FOR THE PETROGENESIS OF LUNAR HIGHLAND SAMPLES

JAMES W. HEAD

Dept. of Geological Sciences, Brown University, Providence, R.I., U.S.A.

(Received 13 May, 1974)

Abstract. The lunar Orientale basin and its associated facies formed as a result of impact into lunar highland crustal rocks. The crater rim is shown to be closely represented by the position of the outer Rook Mountain ring, approximately 620 km in diam. The inner Rook Mountains form a central peak ring within the crater. The 900 km diam Cordillera ring is a fault scarp which formed in the terminal stages of the cratering event as a large portion of the crust collapsed inward toward the recently excavated crater, forming a mega-terrace. This collapse pushed the wall of the Orientale crater inward, distorting it and slightly decreasing its radius.

A domical facies is almost exclusively developed between the Cordillera and outer Rook rings. The domical facies is interpreted to be radially textured ejecta which was disrupted and modified to a jumbled domical texture by seismic shaking associated with the formation of the mega-terrace. The plains and corrugated facies pre-date the mare fill and lie within the Orientale crater. These facies are interpreted to have been deposited contemporaneously with the cratering event as partial and total impact melts which collected on the floor of the crater during the terminal stages of the event. The plains facies, with an estimated thickness of ~ 1 km and a volume of ~ 75000 km^3, represent the most thoroughly impact melted materials which collected and ponded in the central portion of the crater floor. The corrugated facies, with an estimated thickness of ~ 1 km and a volume of ~ 180000 km^3, represent impact partial melts mixed with debris. A relatively small volume of mare material was subsequently deposited in the basin (probably less than 25000 km^3 in Mare Orientale).

There is little evidence that the basin has undergone major structural modifications subsequent to the terminal stages of the cratering event. The striking implication for the Orientale gravity anomaly is that mascon formation may be primarily related to crustal excavation and upwarping of a 'moho' plug, rather than attributable to post-impact mare filling.

The plains units on the floor of Orientale are similar to Cayley-like plains in other multi-ringed basins and on smaller crater floors. Impact melt deposits may therefore be a significant source of Cayley-like plains units.

The volumes of impact melt associated with the Orientale basin and their mode of deposition have important implications for petrogenetic models. Multi-ringed basin formation provides a mechanism for instantaneously melting large volumes of shallow to intermediate depth lunar crustal material which is emplaced such that the differentiation and crystallization of a variety of igneous rock types and textures may occur.

1. Introduction

The lunar Orientale basin is a 900 km diam circular topographic depression covering an area of over 700000 km^2 on the western limb of the Moon (Figure 1a, b). It is the freshest example of a class of lunar craters generally greater than 150 km in diam which form multiple concentric rings (Stuart-Alexander and Howard, 1970; Hartmann and Wood, 1971). The term *basin* refers to the topographic depression defined by the area inside the major scarp associated with the multi-ringed structure. In the case of the Orientale basin, it is the Cordillera Mountains (Figure 2) which define the major scarp, and thus the basin. The Carpathian-Apennine-Caucasus Mountains enclose the

The Moon **11** (1974) 327–356.

Imbrium basin. These basin-defining scarps may or may not represent the original crater rim. The dark material which partially fills the topographic basins is known as mare. Thus, Mare Orientale is a flat, low albedo unit which partially floods and fills the Orientale basin (Figure 1b). Older examples of this type of basin include Imbrium, Serenitatis, Crisium, and Nectaris. There is general agreement on the placement and diameter of the multiple rings of the Orientale basin. There has been no agreement, however, on the placement and size of the original crater rim diameter, with estimates of 100 km (Van Dorn, 1968), 134 km (Van Dorn, 1969), 390 km (Baldwin, 1963; Hartmann and Yale, 1968; Short and Forman, 1972), 480 km (Baldwin, 1969) and 480 or 620 km (Hartmann and Wood, 1971). Understanding of the origin of multi-ring basins is extremely important to lunar studies because their ejecta deposits blanket the

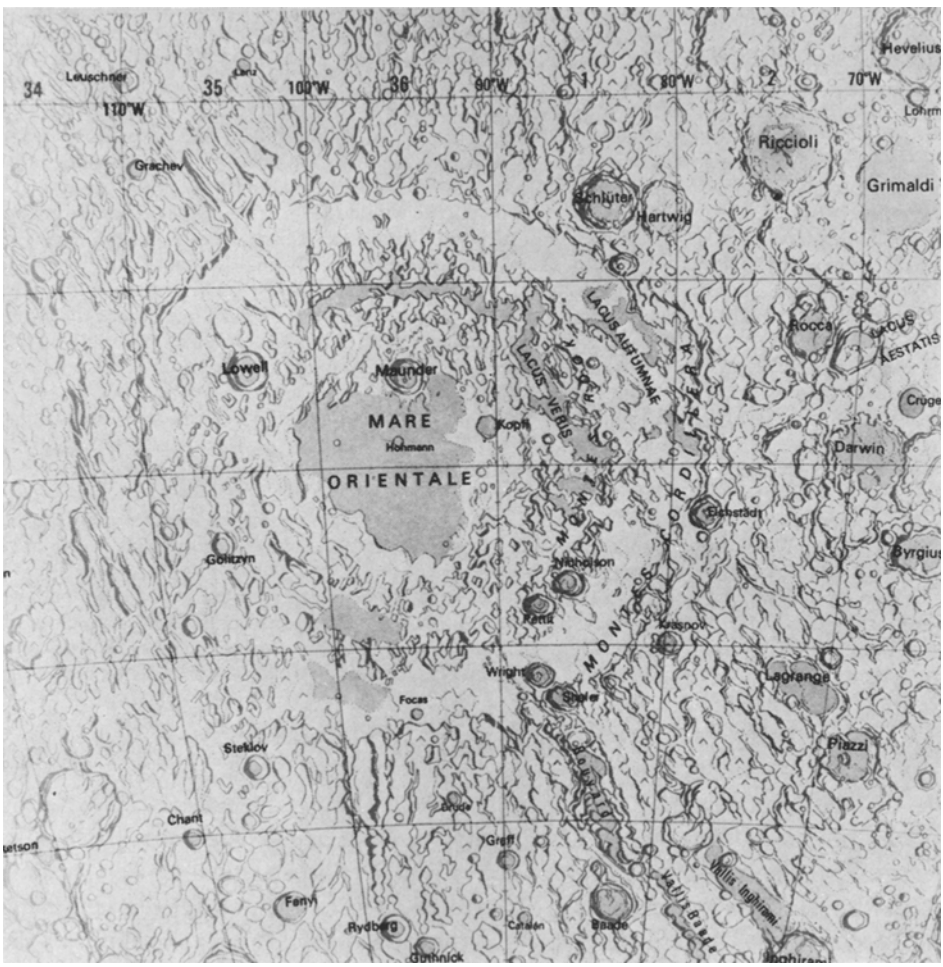

Fig. 1a.

Fig. 1a-b. Orientale basin, about 900 km in diam. (a) Location map (Rükl, 1972). (b) Lunar Orbiter photograph. Portion of LO IV 194M.

Fig. 1b.

Moon, their associated rings form the major lunar mountain ranges, and their interior deposits floor the major mare basins. In addition, two Apollo missions explored a portion of the interior of these basins, Apollo 15 at the edge of Imbrium and Apollo 17 at the edge of Serenitatis.

Previous work on the Orientale basin includes structural, stratigraphic and mapping studies (Hartmann and Kuiper, 1962; Hartmann, 1964; Hartmann and Yale, 1968, 1969; McCauley, 1964a, b, 1967a, b, 1968a, b; Saunders, 1968; Ulrich, 1968, Oriti and Green, 1967; Baldwin, 1972, 1974; Ridpath and Murray, 1970; and Head, 1973a, b, 1974a). A comprehensive geologic map of the Orientale region at a scale of 1 : 5 million is in preparation (Scott, in preparation).

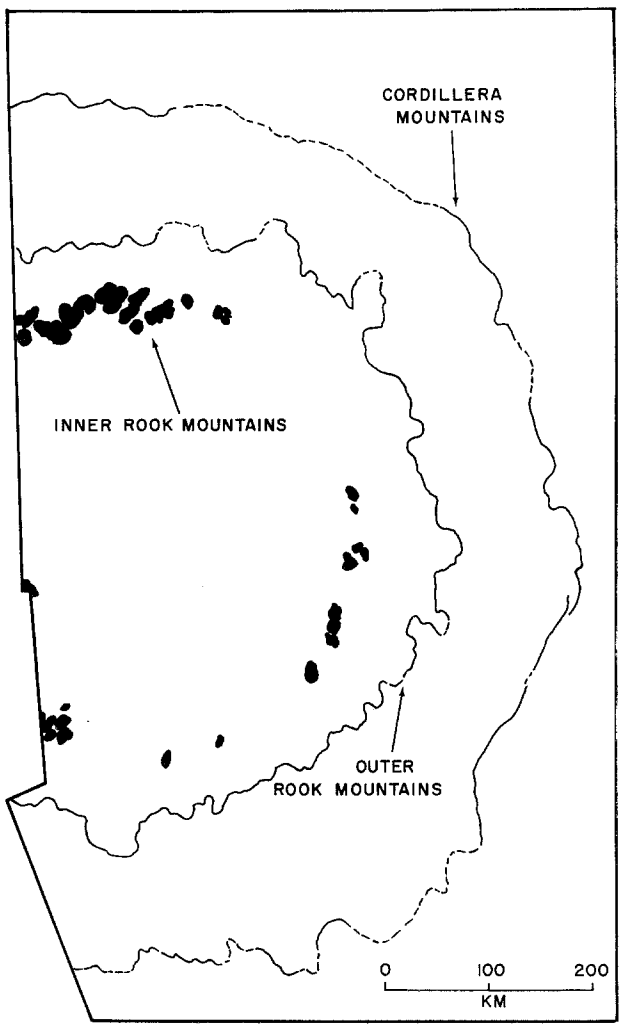

Fig. 2. Orientale basin rings or mountain ranges.

The purpose of this paper is to address several areas, including (1) the definition, distribution, and genetic significance of facies and structures within a major lunar basin; (2) the identification of the original crater within the basin; (3) a model for the origin and evolution of basin interiors; and (4) the implications of this model for lunar sample genesis. An earlier phase of this study was presented elsewhere (Head, 1973b).

Observations with telescopes and study of photographs represent the basic data in this study. Photography includes earthbased telescopic, Russian Zond missions, Lunar Orbiter IV and V, and Apollo 17 earthshine photography. Lunar Orbiter IV obtained high resolution coverage of the central and eastern portions of the Orientale basin and the detailed analysis is therefore concentrated in this area.

2. Orientale Basin Structures

Three major rings are seen in concentric arrangement around the central Mare Orientale (Figure 1, 2). The most conspicuous ring, the Cordillera Mountains (or Eichstadt ring, for a crater on its edge), is about 900 km in diam, and forms the roughly circular scarp which defines the Orientale basin. The next two inner rings together form the Rook Mountains. The outer Rook Mountains form a ring approximately 620 km in diam, while the inner Rook forms a discontinuous ring about 480 km in diam. An inner ring about 320 km in diam is seen at the edge of the maria and forms the depression in which Mare Orientale occurs.

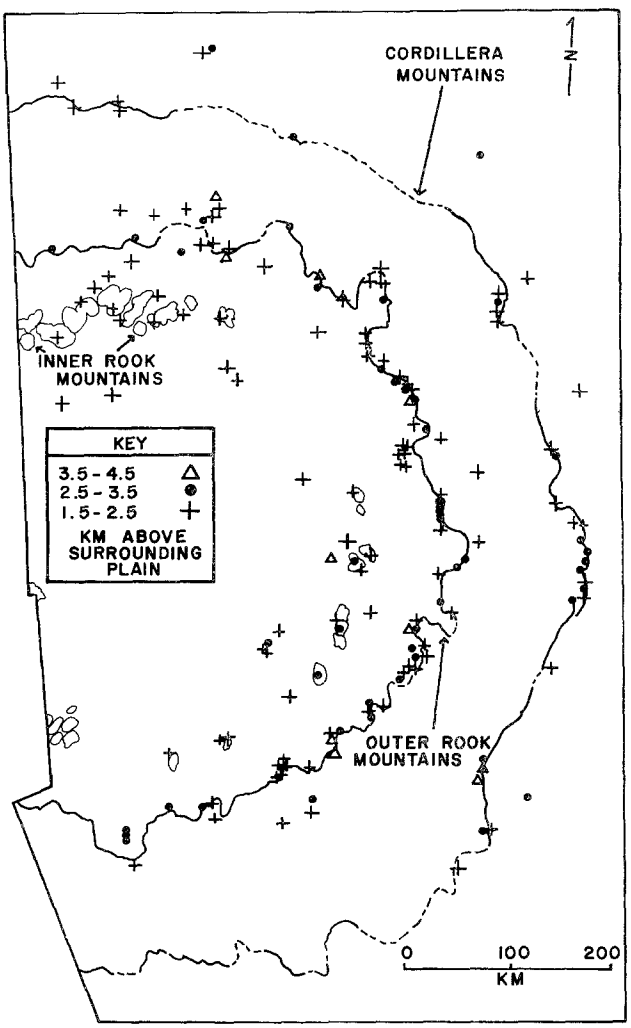

Fig. 3. Heights of selected prominences of the Orientale basin based on shadow measurements. Elevations are in km above surrounding terrain.

2.1. Cordillera ring

The Cordillera ring is a generally continuous scarp which faces toward the interior of the basin. It is of variable height but locally rises to almost four km above surrounding plains (Figure 3). The ring morphology in the south-east portion of the basin is shown in Figure 4 with the radially textured Orientale ejecta blanket to the right of the scarp. The majority of the deposits to the left are representative of the domical facies of the Orientale basin interior. The scarp is of variable height; at the two arrows the height is between 3 and 4 km above the plains. Where the scarp is of lower height, as in the area between the arrows, the radial facies appears to carry through somewhat into the basin interior.

In several places, particularly to the north and south, the Cordillera scarp develops a less linear and more irregular, saw-toothed appearance (Figure 5a, b). This is also seen in the outer Rook ring and is thought to be related to lunar grid patterns in the target rocks prior to the formation of the Orientale basin, (Head, 1974c, Figure 22). The regional lunar grid is oriented in a NW–SE, NE–SW pattern in this area and thus intersects in a sawtooth pattern at points where these trends converge (particularly to the north and south), while producing more linear segments where the basin edges are parallel to major trends (NW, SE, etc: see Figures 4, 5a, b).

The linearity and sharpness of the Cordillera ring and its relation to lunar grid structures suggest that it represents a major fault scarp with the interior of the basin displaced relatively downward. Sharpness of the scarp and lack of evidence of debris piled up along the scarp suggests that it formed after the outward movement of ejecta associated with the impact event.

2.2. Outer rook ring

The outer Rook ring (Figure 2, 6) is composed of a generally continuous series of massifs which form an irregular or angular ring, while the inner Rook is outlined by a discontinuous ring of single peaks or groups of peaks. The outer Rook ring is a continuous scarp consisting of a series of 2–20 km diam massif blocks with their steep slopes facing the basin interior and their shallow slopes dipping away from the basin. The linear elements in the outer Rook ring generally parallel linear elements in the Cordillera scarp (Figure 2). The ring height is variable but ranges up to about 4 km. The massifs seen here average between 1.5 and 3.0 km. The outer Rook ring separates the domical facies (to the south in Figure 6) from the basin interior.

2.3. Inner rook ring

The inner Rook ring is formed by isolated peaks or groups of peaks, as indicated at the arrow in Figure 6, and these range from 2–10 km in width and are up to 3 km in elevation, but generally average about 1 km in height. They stand in contrast to the scarps forming the outer Rook and Cordillera rings in their shape and continuity (Figure 2).

The morphology of the inner and outer Rook rings bears strong resemblance to crater morphology in lunar craters ranging from 75 to 350 km in diam. Craters below

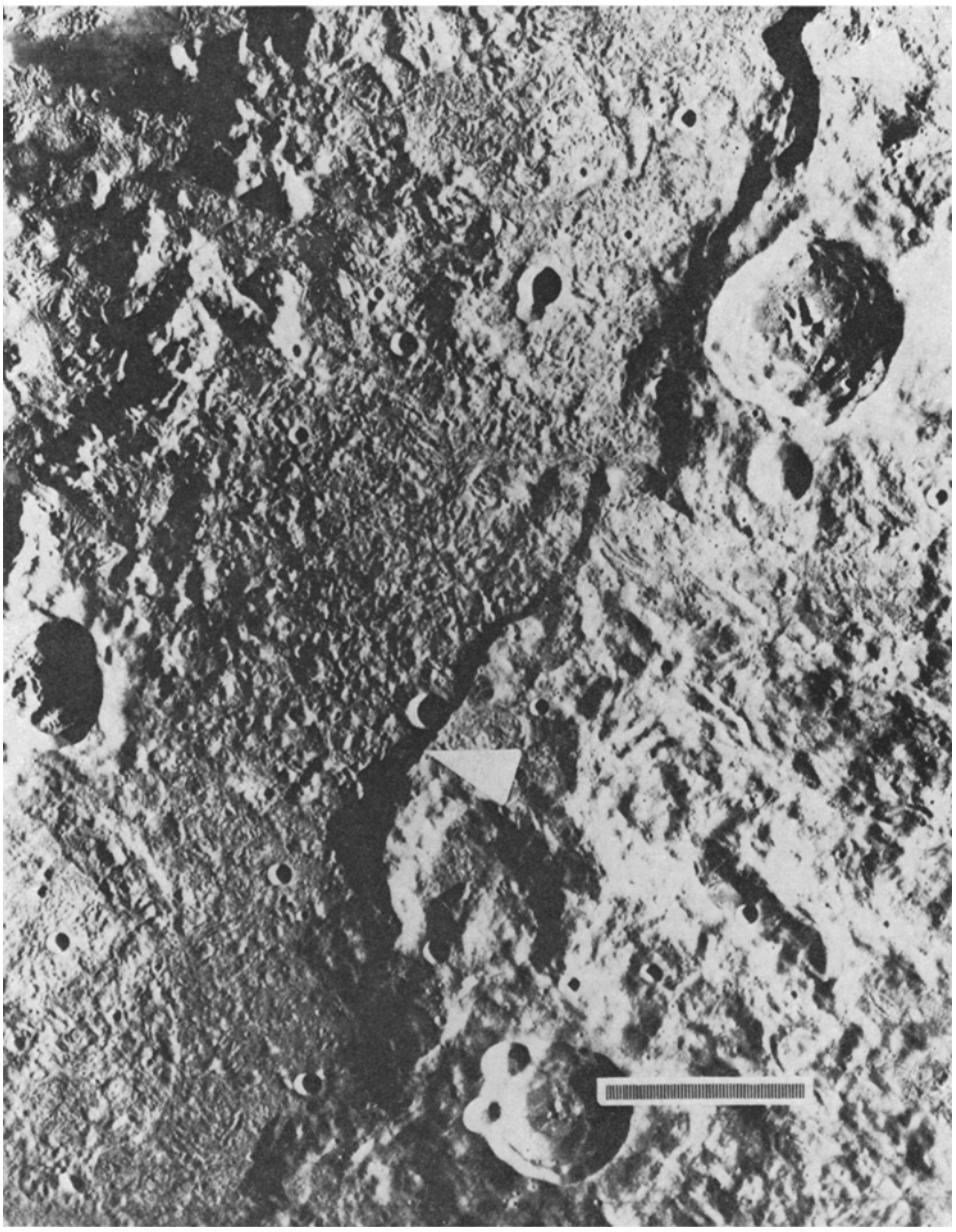

Fig. 4. Southeastern edge of the Orientale basin. Inward-facing Cordillera scarp separates radially textured ejecta to the right from domical facies to the left. Scale bar is about 50 km. LOIV 181H1.

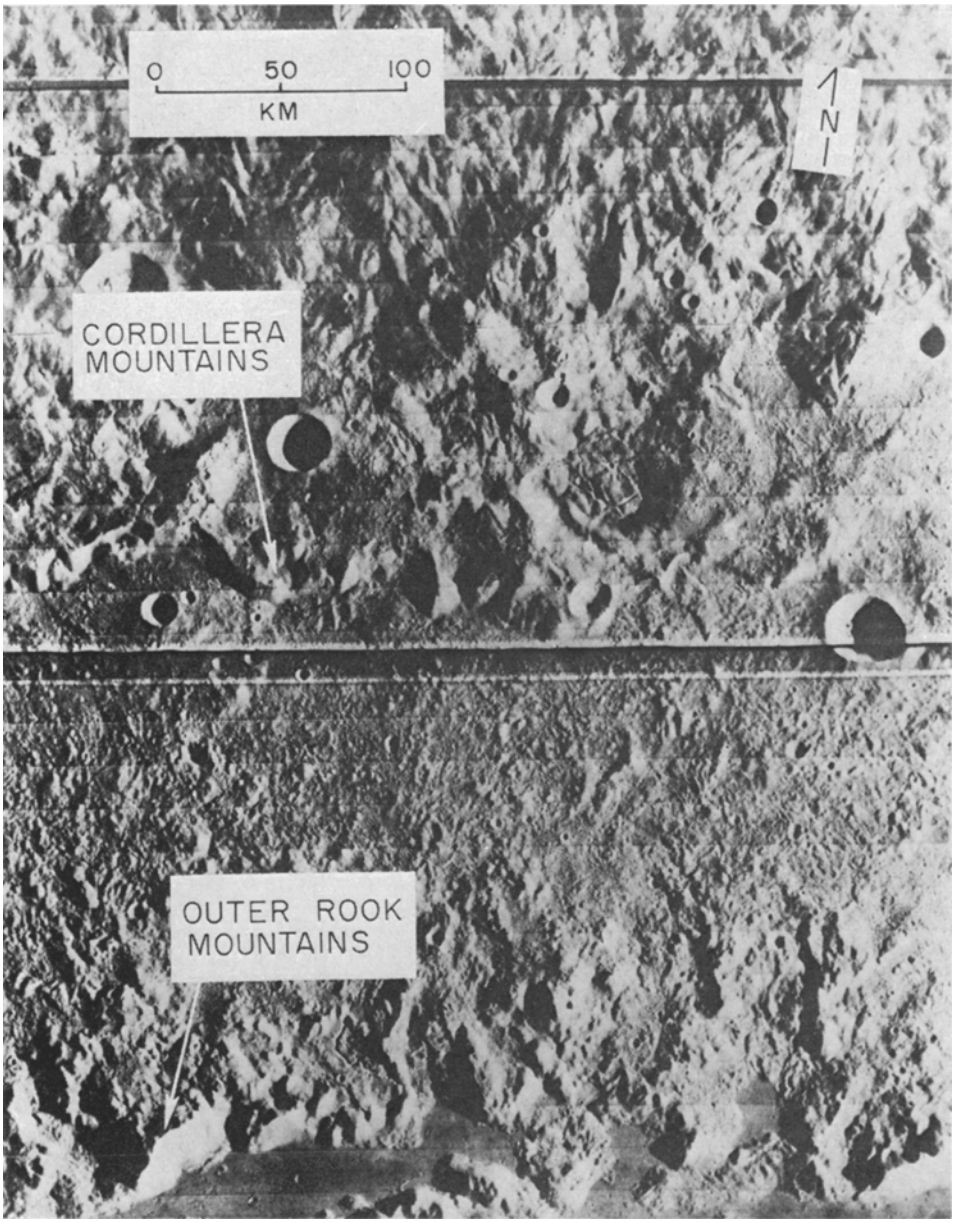

Fig. 5a.

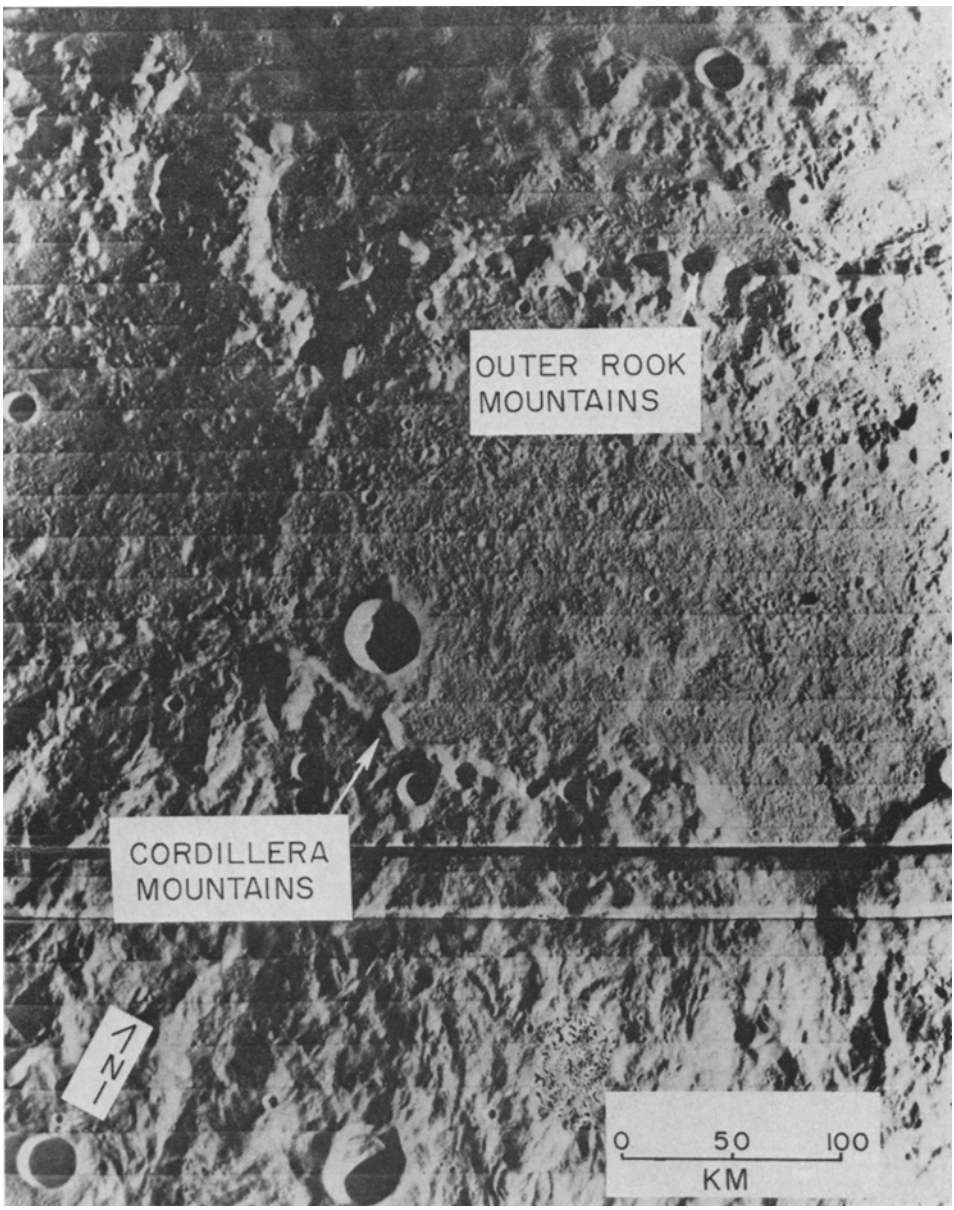

Fig 5b.

Fig. 5a-b. Irregular patterns in the Cordillera and Outer Rook Mountains related to pre-existing structure. (a) Northern edge of the Orientale basin. LOIV 195H3. (b) Southern edge of the Orientale basin. LOIV 194H3.

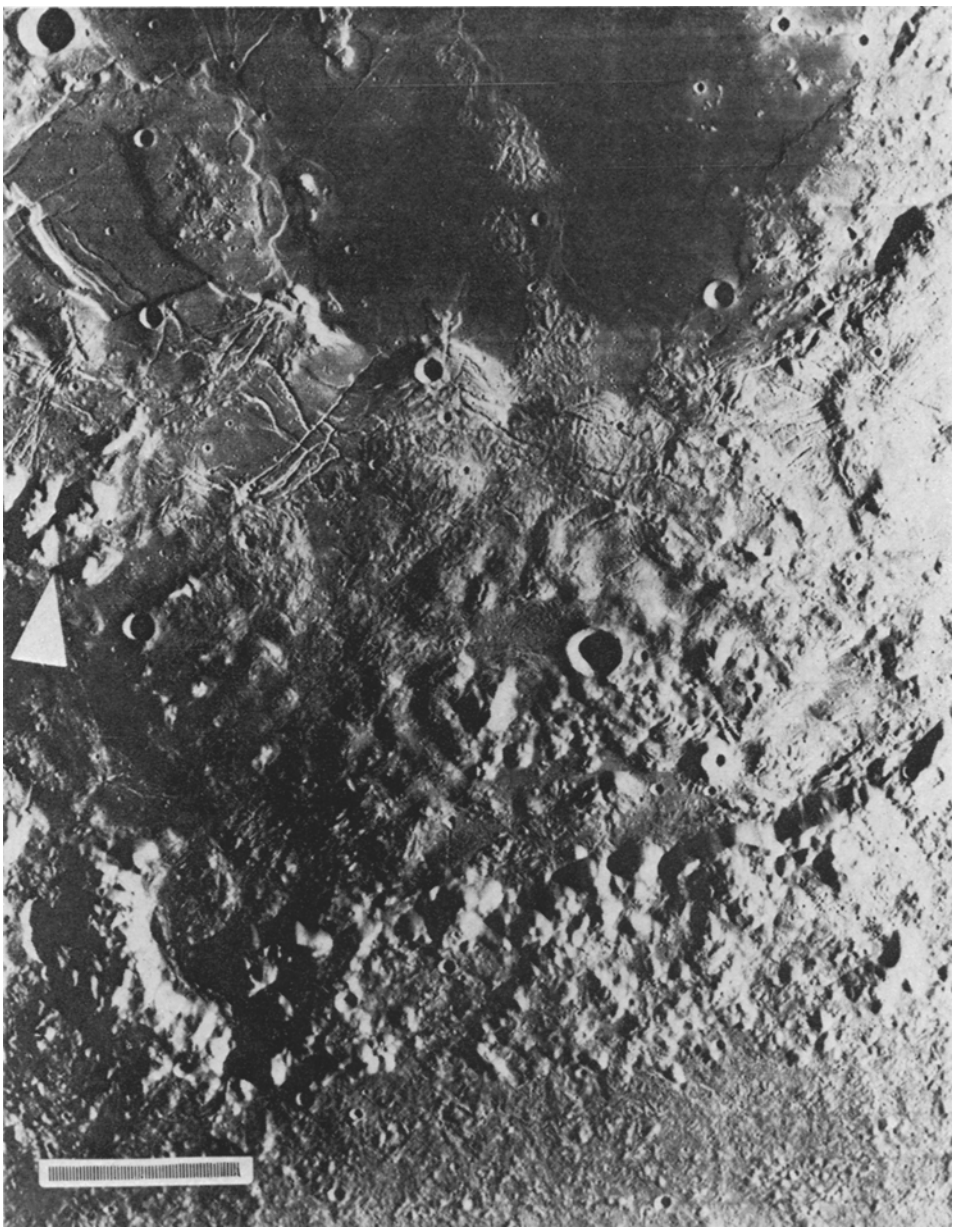

Fig. 6. Outer and inner Rook rings in the Southern Orientale basin. Inward facing outer Rook ring separates domical facies at base from corrugated and plains facies to the north. Arrow points to group of peaks making up part of inner Rook ring. Scale bar is about 50 km. LOIV 195H1.

about 130 km in diam are characterized by terraced crater walls and an isolated central peak or group of central peaks. Hartmann and Wood (1971), Hartmann (1972), and Wood (1968, 1973) have described the configuration of central peaks with increasing crater diameter, showing that they progress through a stage of increasing size, become multiple, and then grade into a central peak ring (a ring of peaks on the crater floor usually at about half the crater radius). Two craters showing similarities to Orientale rings are illustrated in Figure 7. The 170 km diam crater Hausen (Figure 7a) is characterized by a terraced crater wall and the sharp crater rim is the uppermost inward-facing fault scarp of this series of terraces. The larger Schrödinger basin (320 km diam; Figure 7b) is intermediate in size between Hausen and Orientale and still maintains the characteristic terraces and fault scarps of the crater wall. The central peaks of the crater Hausen show an interesting combination of a massive group of central peaks and a smaller incipient central peak ring. Schrödinger, on the other hand, shows a well-developed 155 km diam central peak ring. The discontinuous central peaks and central peak rings are clearly distinguishable from the continuous terraced fault scarps of the crater wall.

Analysis of the Orientale rings (Figure 1, 2) shows that the inner Rook ring closely resembles the central peaks and central peak rings of Hausen and Schrödinger. The outer Rook ring is similar to the inward facing fault scarps of the crater wall terraces of smaller craters (Figure 7a, b). The Cordillera ring is also similar to crater wall terrace fault scarps but an analogous ring is not seen in smaller lunar craters. Based on Orientale basin ring distribution and comparative morphology, a tentative conclusion is that the inner Rook ring is a central peak ring of the original Orientale crater and that the next outer ring (outer Rook) represents the approximate crater rim. However, the Cordillera ring cannot be ruled out as the approximate crater rim on the basis of morphologic evidence alone.

The Orientale basin departs radically in detail from the circular form of smaller craters. The major structural lineaments associated with Orientale (Figure 8) appear to be related to a regional pre-Orientale grid system which affected the shape of the basin both in terms of initial excavation and subsequent structural modification.

3. Orientale Basin Deposits

The deposits of the Orientale basin interior can be subdivided into various units or facies based on their morphologic characteristics (Figure 9). The basin interior is surrounded by facies of the textured ejecta blanket which occur almost exclusively outside of the Cordillera ring (Head, 1973a).

3.1. Domical facies

The domical facies is characterized by 1–5 km diam, generally equidimensional, rounded domes which appear randomly distributed. The domical facies occurs almost exclusively between the Cordillera scarp and the outer Rook ring. Where the Cordillera scarp is steep, the domes are usually random and well developed. Where the Cordillera

scarp is poorly developed, as between the two arrows in Figure 4, the elements of the domical facies have a linear aspect which is radial to the basin and similar to patterns of ejecta deposited outward from the Cordillera scarp. This lateral continuity, which is seen in several regions around the basin interior, suggests that the domical facies was originally related to the radial ejecta patterns, but that it was subsequently modified to produce the randomness characteristic of the rest of the domical facies. In addition, several large crater forms and a possible extension of a crater chain (Figure 8) can be seen between the outer Rook and the Cordillera ring, further suggesting that this area was originally blanketed rather than being within the crater of excavation. This major development of domical facies (Figure 9) does not have a counterpart in smaller craters. Based on these observations, the following model is proposed for the origin of the domical facies.

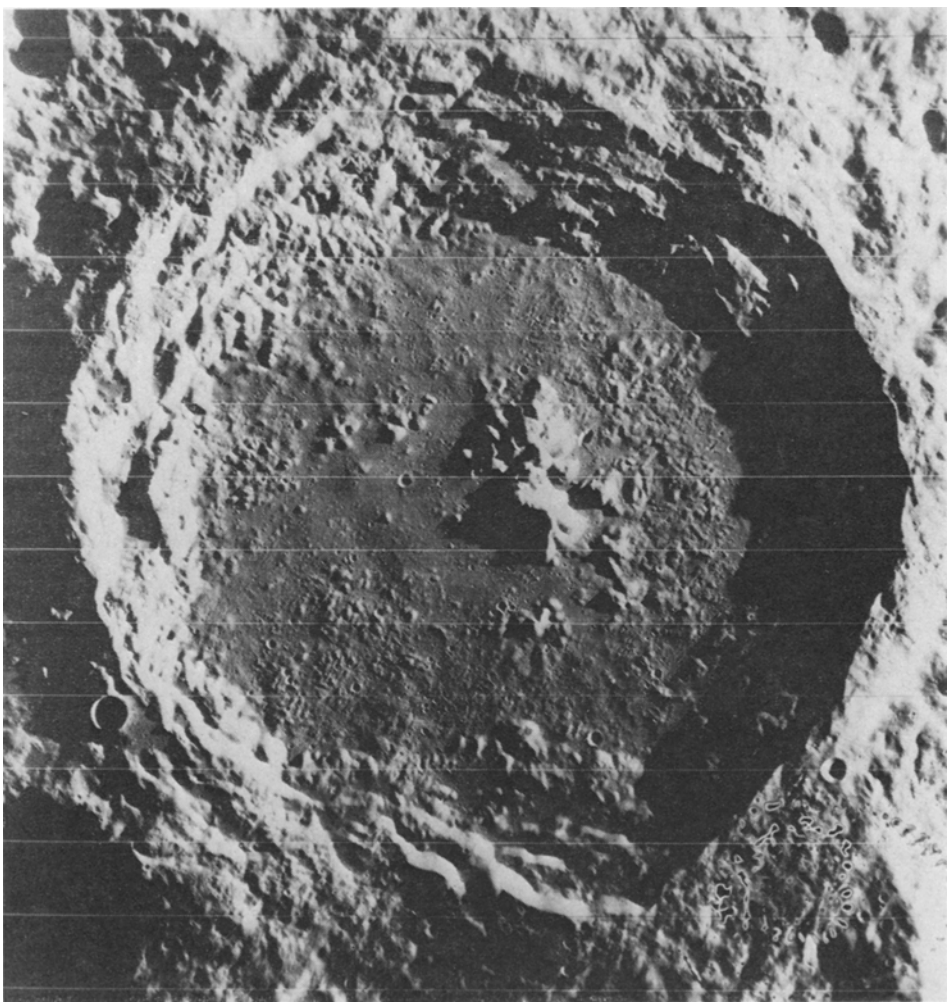

Fig. 7a.

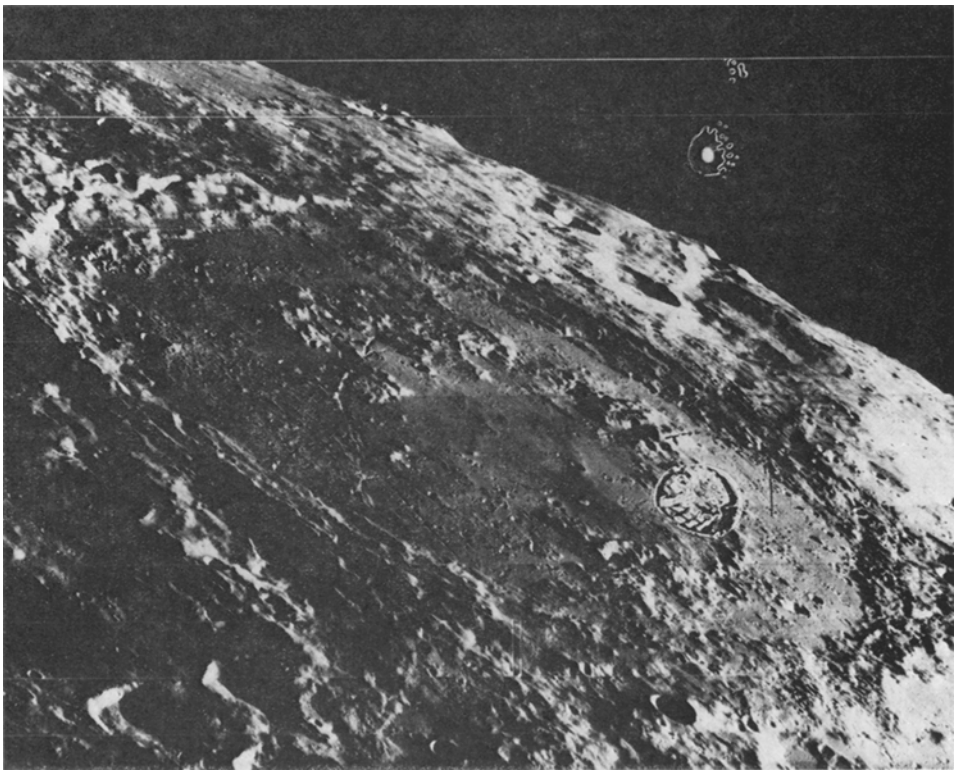

Fig. 7b.

Fig. 7a–b. Craters showing structures and features analogous to those in Orientale. (a) Hausen, 170 km diam; LOIV 193H2. (b) Oblique view of Schrödinger, 320 km diam. Central peak ring is 155 km diam. LOV 21H2.

The Orientale cratering event excavated material from the crater and spread it out in radial patterns away from the outer Rook Mountains, the apparent crater rim. Thus, before the formation of the Cordillera scarp, the radial pattern extended through the area now occupied by the domical facies (Figure 10a) and is still seen in part (Figure 4). After radial movement of ejecta ceased in the terminal stages of the cratering event, the rim tended to slump inward toward the newly excavated crater. Factors responsible for the inward movement may have included shock wave rarefaction, the additional mass (ejecta) on the crater rim, or simply collapse toward a newly excavated depression. This inward movement resulted in the formation of the Cordillera scarp (Figure 10b) which represents the fault plane along which this major portion of the crust moved downward and inward toward the crater. The formation of this fault, and the associated seismic shaking and change in slope is believed to be the factor responsible for the general modification of the radial patterns of the recently deposited ejecta blanket. The radial structure was least disturbed in the areas where there was least offset on the Cordillera scarp. The exact cause of the domical form is not

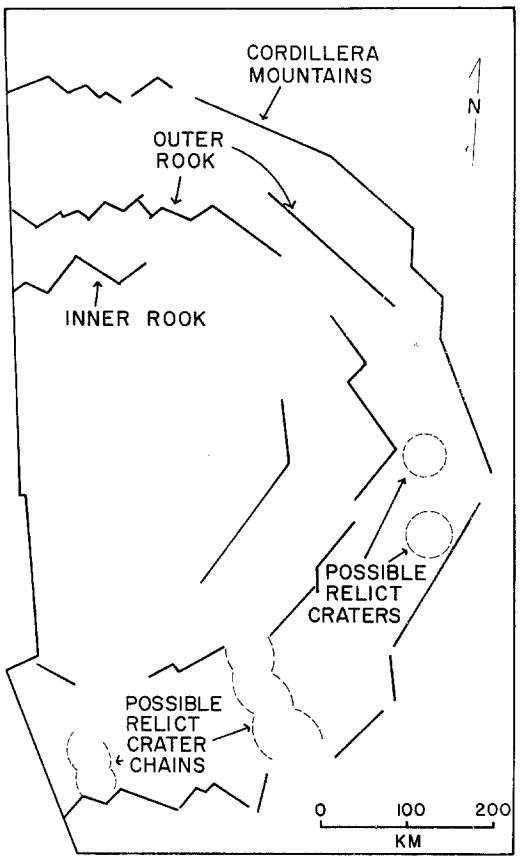

Fig. 8. Major structural lineament patterns in the Orientale basin and possible relict craters and crater chains in the domical facies region.

understood. It is hypothesized, however, that the material on the rim is composed of large blocks of ejecta deposited on the crater rim at low velocities. The seismic shaking associated with the formation of the Cordillera scarp caused the finer material to be shed off these km-sized blocks, enhancing their topographic expression and causing the development of the dome-like structure. Areal distribution and size distribution studies of the domical facies are presently underway to test this hypothesis. Whatever the detailed origin of the domes, the faulting model provides a mechanism to explain the presence of the Cordillera scarp, the restricted distribution of the domical facies, and the modification of the radial facies between the Cordillera and the Rook Mountain range.

A small patch of domical facies has been mapped outside the Cordillera scarp at the northern edge of the basin (Figure 9, 11). This patch appears anomalous in that the domical facies is usually restricted to the area between the Cordillera and outer Rook ring. This anomalous distribution is believed to be due to the fact that the Cordillera fault transected two pre-existing major blanketed craters in this region leaving 'hanging

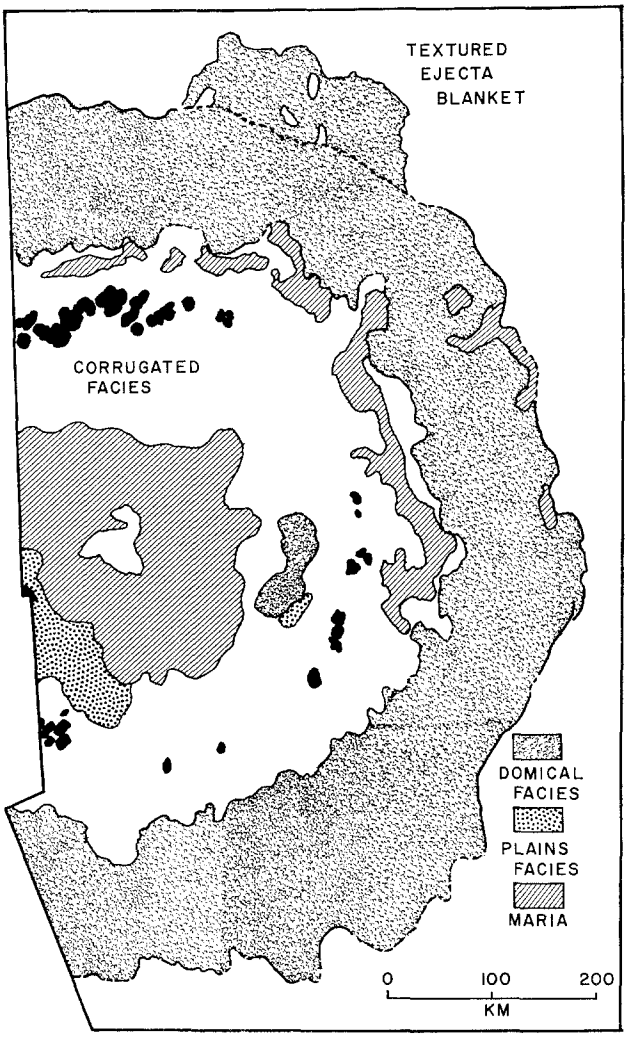

Fig. 9. Facies of the Orientale basin.

valleys' pointing toward the crater interior. Material within these craters, in turn, tended to move toward the basin interior, undergoing deformation similar to the domical deposits between the outer Rook and Cordillera rings (Figure 11).

3.2. Corrugated facies

The surface of the corrugated facies (Figure 12) has a pitted texture which is laced with surface cracks ranging in width from the limits of resolution up to about 2 km and up to tens of km in length. The corrugated facies is often developed on broad elongate ridges and the larger surface cracks are often at the crest of these ridges as shown at the upper arrow in Figure 12. The broad ridge structures are thought to represent underlying topography because in many places peaks of non-corrugated material

protrude through the facies, as seen at the lower arrow in Figure 12. These characteristics suggest that the corrugated facies is material draped over pre-existing topography, as shown in Figure 13. Crestal furrows are often developed where the material is draped over pre-existing ridges. The pitted and cracked nature of the surface is attributed to cooling and contraction similar to that seen in molten deposits such as lavas. In the case of Orientale, the corrugated facies is restricted to the interior of the outer Rook ring (Figure 9). In smaller fresh craters such as Tycho, Aristarchus, and Copernicus, materials of similar morphology are distributed on the crater floor within the crater rim. This adds support to the earlier tentative conclusion that the outer Rook ring approximates the original crater rim. The corrugated facies is thus interpreted to be partially shock-melted materials which have fallen back and slid into the crater and blanketed the crater interior, cooling to form the pitted and corrugated facies. The area covered by the corrugated facies within Orientale is about 180000 km^2.

3.3. Plains facies

The plains within Orientale are generally of intermediate albedo and regionally smooth, although cut by numerous fractures (Figure 6). The plains cover an area (including that underlying the maria) of about 75000 km^2. They lie in marked contrast to the rougher texture of the corrugated facies. Plains deposits are embayed by the dark maria but are intimately related to the corrugated facies, as shown by gradational contacts and by the through-cutting relationships of cracks and furrows in both

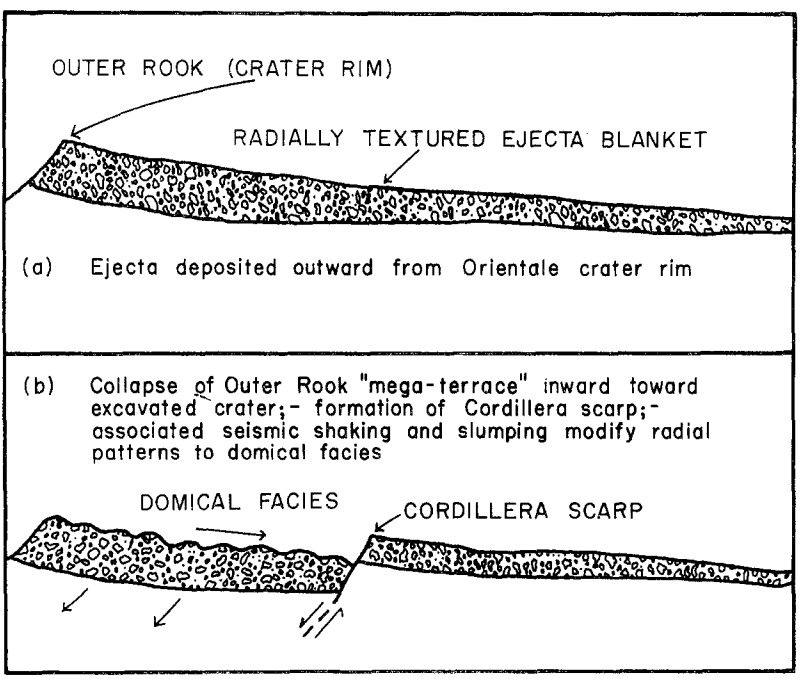

Fig. 10. Model for the formation of the Cordillera scarp and associated features.

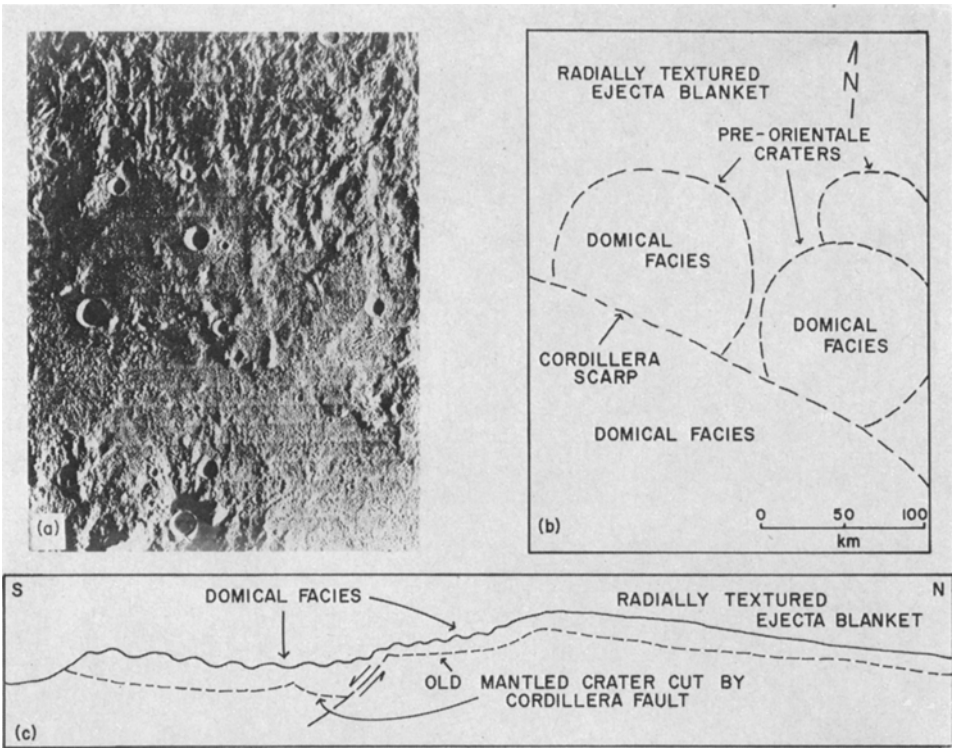

Fig. 11. Development of domical facies on Orientale basin rim by faulting of pre-Orientale ejecta-filled craters. (a) Northern Orientale basin rim, LOIV 187H3. (b) Features shown in (a). (c) Cross-section showing faulting of old crater, creation of 'hanging valley', and deformation of crater fill into domical facies.

facies (Figure 6). Cracks which originate in the corrugated facies can be followed into the plains where they widen. The majority of cracks and furrows associated with the plains and corrugated facies appear to be related to shrinkage, cooling and draping of molten and semi-molten material over pre-existing topography, rather than tectonic adjustment subsequent to the formation of the crater and its associated deposits.

The cracks and furrows are unevenly distributed but are generally concentric or radial to the basin (Figure 14a, b) and are concentrated in areas of rough underlying topography or around the edge of the innermost depression. These cracks are morphologically dissimilar to the few larger grabens (Figure 14a, b) which are relatively younger (but still pre-mare) and which appear to represent deformation of the whole deposit rather than shrinking or draping of a portion of it. Many structures analogous to the cracks and furrows are seen on terrestrial lava flows, such as drainage features, pressure ridges, or where flows are draped over pre-existing topography (Green and Short, 1971, plates 110A, 121A–B, 131A–B). Similar structures are seen on regional cooling units such as ash-flow tuffs (Ross and Smith, 1960; Sheridan, 1970) and are related to contraction due to cooling and degassing of the sheet.

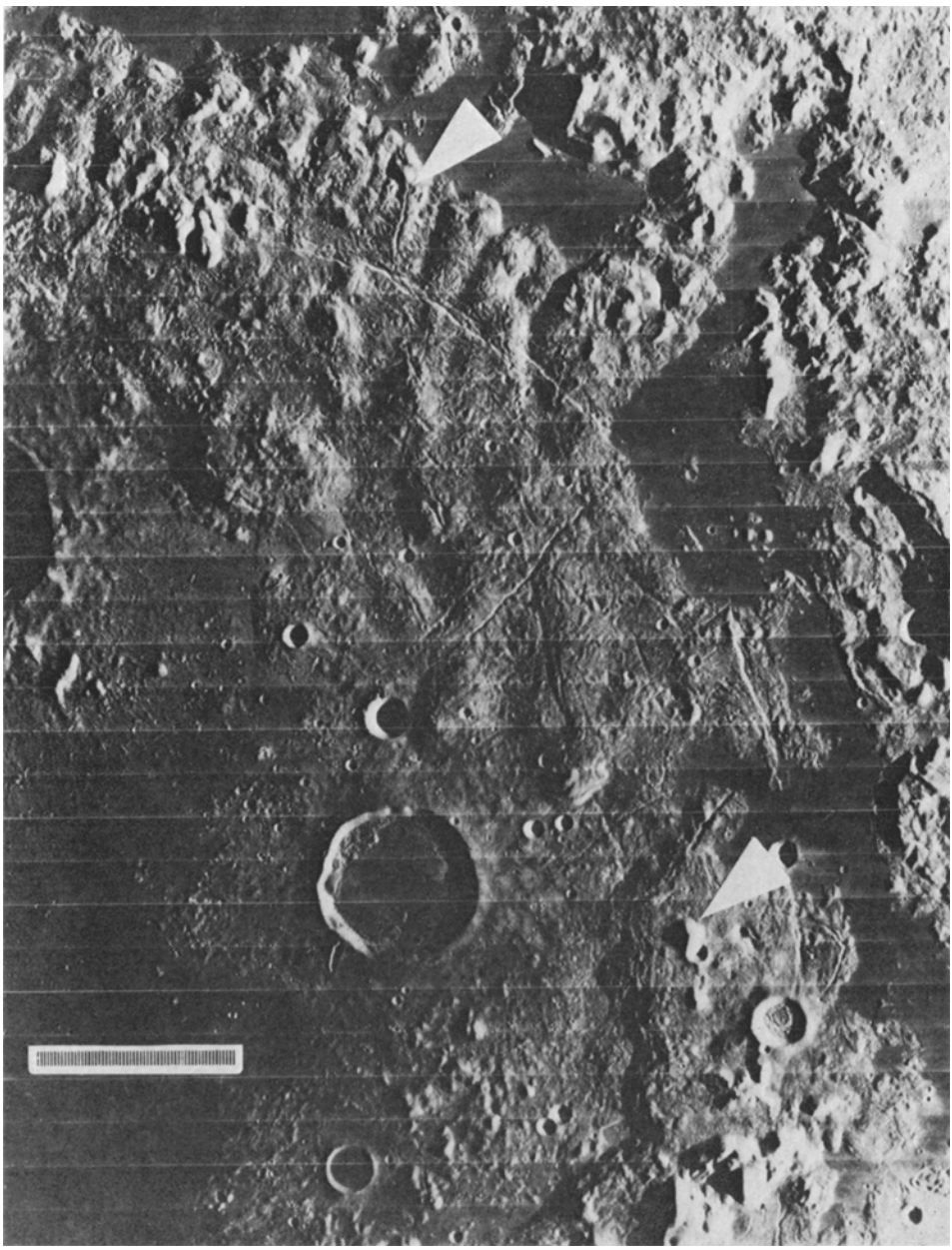

Fig. 12. Corrugated facies in northeastern Orientale showing characteristic pitted and cracked appearance of surface. Upper arrow indicates surface crack at crest of underlying hill. Lower arrow indicates peak of inner Rook ring protruding through corrugated facies. Scale bar is about 50 km. LOIV 187H2.

Considerable work has been done on the presence and distribution of impact melts in terrestrial impact craters (Dence, 1964, 1965, 1968, 1971; Beals, 1965; Short, 1965, 1970; and others) and much of this work is summarized in French (1970), Dence (1971), and Engelhardt (1972). Impact melted rock occurs in two major modes in terrestrial impact craters: (1) as crystalline matrix of breccias and as glassy fragments, and (2) as

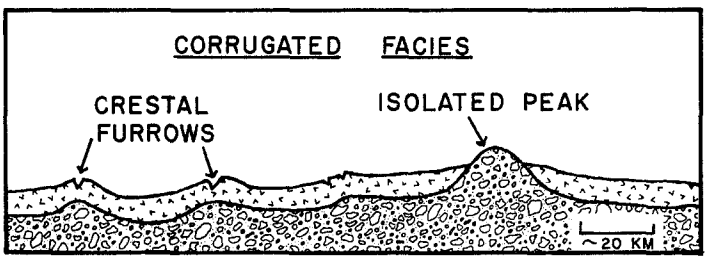

Fig. 13. Schematic cross-section of corrugated facies showing probable relation of corrugated facies to underlying topography.

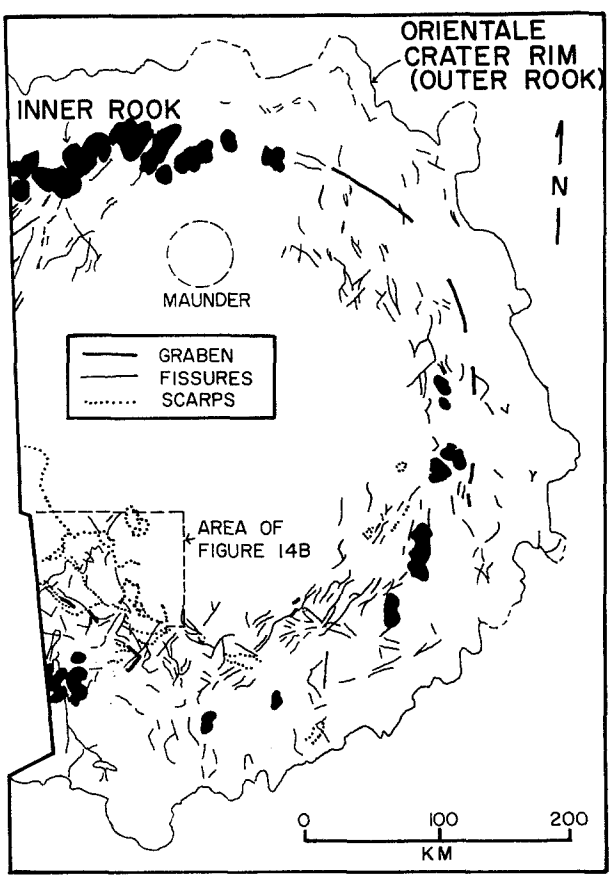

Fig. 14a.

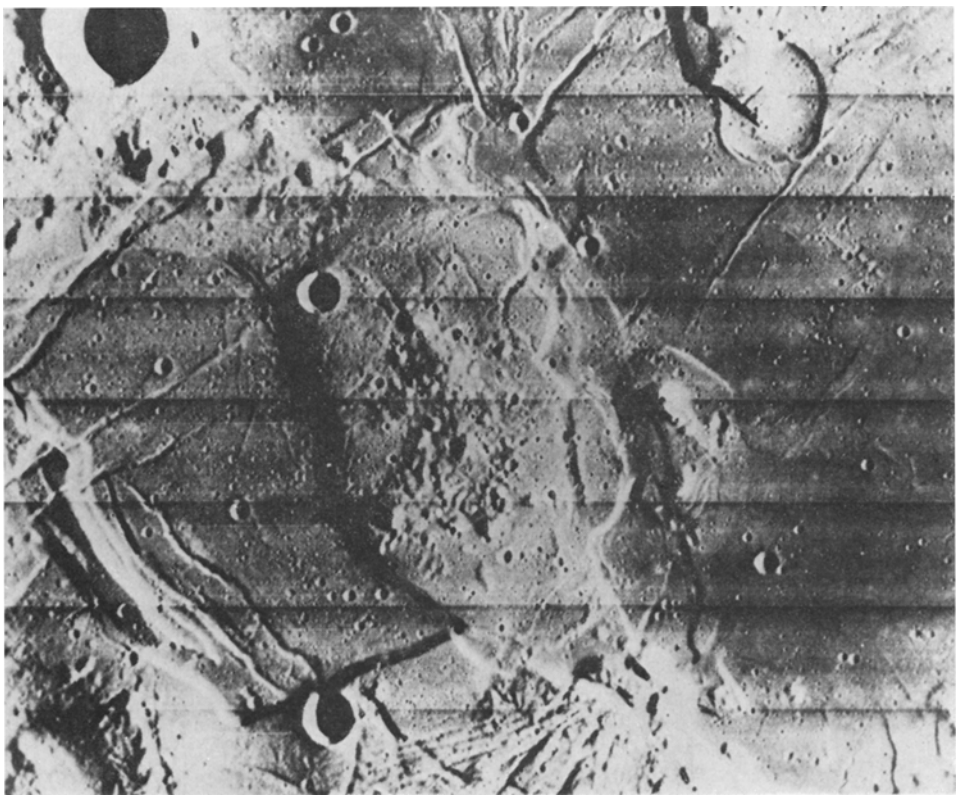

Fig. 14b.

Fig. 14a-b. Structure and texture of Orientale crater floor deposits. (a) Graben, and fissures and scarps associated with plains and corrugated facies. Discrepancy in north due in part to modification by young crater Maunder. (b) Fissures and scarps in plains deposits at edge of Mare Orientale. Framelet width is 11 km. Portion of LOIV 195H1.

discrete layers of melted rock which are completely recrystallized and resemble igneous rocks. In small, simple craters (Dence, 1968) a melt layer generally occurs at the low point in the center of the crater below the breccia lens. In larger, complex craters (Manicouagan, Clearwater Lakes; Dence, 1965, 1968), the melt layer forms an annular ring on the surface between the central uplift and the rim and may be as much as several hundred meters thick (French, 1970).

Based on the surface morphology, mode of occurrence, fracture system, and fracture size, the corrugated facies and plains are interpreted to be contiguous portions of crater interior impact deposits containing variable amounts of shock-melted material. The smooth surface, large crack size and abundance, preferential deposition in lows and location in the basin center, all argue that the plains units were the most fluid and contained the highest proportions of shock-melted materials. The rougher textured surface, smaller cracks, and draped nature of the corrugated deposits argue that this

facies was less fluid but still contained molten material, probably mixed with varying proportions of non-molten to partially-melted ejecta. The intimate association and gradation of the two facies and their structures argues for their contemporaneity, and their distribution within Orientale indicates that they formed during the cratering event.

3.4. Maria

An additional unit occurs within the Orientale basin in the form of a low albedo, smooth deposit similar in albedo and morphology to the basaltic lava flows sampled on Apollo missions. These maria are located in the central portion of the basin (Mare Orientale, about 50000 km^2, Figure 9), along the base of the outer Rook, (Mare Veris, about 12500 km^2), and along the base of the Cordillera (Mare Autumni, about 5000 km^2). There is a definite asymmetry in the presence of maria along the base of the scarps with the vast majority concentrated in the northeast quadrant toward Oceanus Procellarum. The maria surfaces can be differentiated from the adjacent plains in that they are not cut by the fracture systems characteristic of the corrugated and plains facies. In fact, the maria overlap and embay the domical, corrugated, and plains facies indicating that the maria were deposited at a later time. In addition, the maria show very little sign of deformation other than wrinkle ridges.

4. Sequence of Formation of Structures and Deposits

Based on the characteristics and relationships of Orientale basin structures and facies the following sequence of events is hypothesized (Figure 15, 16):

(1) The Orientale region prior to the formation of the basin was a heavily cratered area similar to the region to the north. A large basin (SE limb basin, 480 km diam;

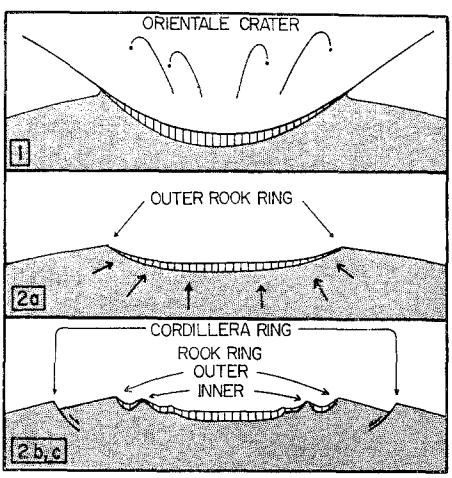

Fig. 15. Excavation and modification stages during the Orientale cratering event. Vertical ruling indicates partially to completely shock-melted material. In part after Dence (1968).

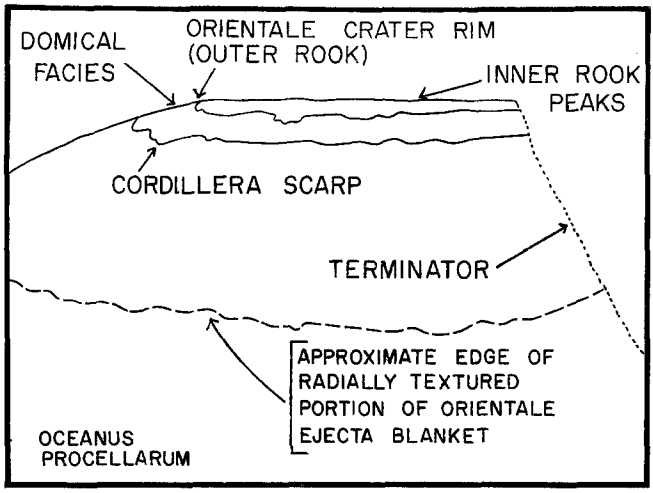

Fig. 16a.

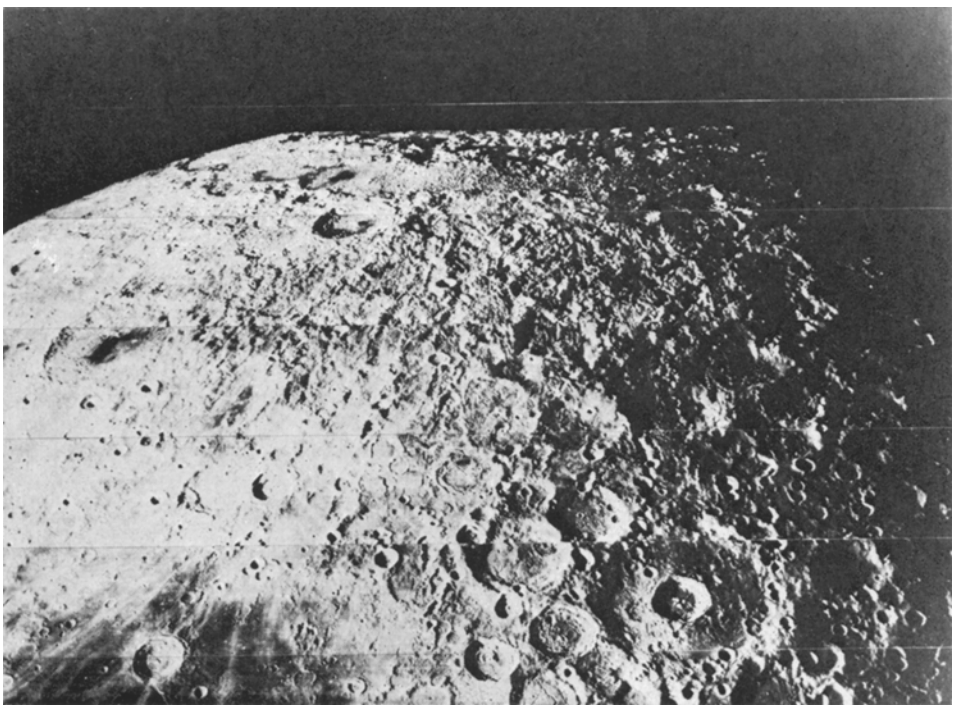

Fig. 16b.

Fig. 16a–b. Edge of the Orientale basin in relation to the curvature of the Moon. Note the small disruption at the Cordillera scarp. Top of photo is cropped and does not represent the continued curvature or edge of the Moon. LOIV 183M. View is from north to south.

Hartmann and Wood, 1971) existed to the south of the present site of Orientale and was surrounded by ejecta deposits. The crust in the Orientale area contained regional structural inhomogeneities along NE and NW oriented 'lunar grid' directions. This is indicated because all subsequent deformation trends in these directions.

(2) Approximately 3.85 billion years ago (Schaeffer and Husain, 1974) a large extra-lunar body impacted the surface in this region and formed a transient cavity, the edge of which most closely approximates the outer Rook ring in position. An ejecta blanket was deposited from the rim of the crater (outer Rook ring) outward. Molten and partially molten shock-melted materials lined the interior of the cavity and began settling to the crater floor as the final crater began to take shape. The formation of the Cordillera scarp took place subsequent to the last stages of rim ejecta deposition since no ejecta appears to have impacted into or banked against the scarp. Hartmann and Wood (1971) suggest that these outer rings may have formed significantly after interior rings. Baldwin (1972) argues on the basis of crater densities that the rings formed at approximately the same time. Evidence presented here indicates that the Cordillera scarp formed as a part of the transition of the transient cavity to the final crater. The primary evidence for this is the observation that the corrugated and plains facies (interpreted to be partially to wholly melted deposits lining the crater interior) do not show evidence of structural deformation which would accompany formation of a massive ring fault such as the Cordillera ring. Instead, the crater deformation associated with the formation of the Cordillera ring (primarily the inward movement of the crater walls and possibly the formation of the central peak ring) appears to be draped and blanketed by the corrugated and plains facies, suggesting that this deformation took place during structural equilibration of the transient cavity but prior to the final settling and cooling of the shock-melted deposits. The formation of the Cordillera ring is thus interpreted to be similar to the formation of terraces in smaller craters, such as Copernicus. These form by slumping of the crater walls into the transient cavity after the initial shock waves have passed and as the region around the crater adjusts to the presence of the cavity. That these terraces form during the event is also evident from the pools and drapings of partially molten shock-melted material that superpose the slumped terraces. Also, the linear portions of the irregular ring structure of the outer Rook ring (Figure 2, 8) parallel major linear portions of the Cordillera ring, suggesting that downfaulting of the Cordillera blocks pushed the original crater rim somewhat inward, slightly decreasing its diameter. The area between the Cordillera ring and the crater rim (outer Rook) might then be viewed as a 'megaterrace' whose formation is intimately associated with the formation of the primary crater. It is interesting to note that in smaller craters we identify the edge of the crater as the outermost scarp. Therefore, as is well known, this always overestimates the diameter of the transient cavity. With a megaterrace situation, we are identifying not the outer slump scarp (Cordillera) but the approximation of the original crater rim (outer Rook). If the above model is correct, then a measurement of the present diameter of the outer Rook ring *underestimates* the actual crater rim because the actual crater rim has been pushed inward and slightly decreased in diameter by the formation of the Cordillera

scarp. This deformation is of the original crater rim as is seen in Figure 8 and parallels the Cordillera scarp directions.

(3) The formation of the Cordillera scarp also deformed the ejecta deposits on the Orientale crater rim into a domical facies in the manner described previously. Since the Cordillera scarp formed during the terminal stages of the cratering event, the ejecta was probably still hot, and thus more easily deformed. This mode of formation differs from that of Baldwin (1972, 1974) who envisions that this portion of the basin was fluidized by tsunami-like waves radiating outward from the crater and released by the impact. Baldwin cites the lack of buried craters in this zone as evidence that the whole region was fluidized. It is unclear why the fluidized region should be confined to the interior of the Cordillera ring and should stop so abruptly. In addition, there appear to be some remnants of pre-existing craters between the Cordillera and outer Rook rings (Figure 8). The deformation of the domical facies and its position within the Cordillera ring seem more easily explained by deformation associated with the mega-terrace formation and inward collapse of the Orientale crater than by the tsunami model of Baldwin (1972, 1974).

(4) Subsequent to the formation of the present crater floor and the cooling and cracking of its deposits, dark mare material flooded portions of the floor of the Orientale basin. Hartmann and Yale (1968, p. 137) suggest that the weight of this added mare fill caused the inner basin to downbuckle and formed concentric rilles. However, the observations and relationships outlined here show that the basin ceased downwarping soon after the crater was formed and that virtually all fractures, faults and rilles are *flooded* by the maria. Hartmann and Yale (1968) note that crater densities for Veris and Autumni are significantly higher than those for Mare Orientale and are very close to those for the ejecta blanket. They cite this as evidence for the early formation of maria along the rings followed by extrusion into the central part of the basin. Another possible explanation for the near-contemporaneity of Veris-Autumni and the ejecta blanket is that these ring-associated pools are actually pools of shock melt concentrated in lows at the base of the scarps, similar to smaller scale shock-melt terrace pools commonly seen in young terraced craters such as Copernicus, Tycho and Aristarchus.

5. Summary and Discussion

(1) The *Orientale basin* is composed of a series of structures and facies which are related in time and mode of origin to the formation of a major impact crater approximately 620 km in diam.

(2) *Crater diameter* – Based on morphologic evidence and comparison to smaller craters, the outer Rook Mountain ring, about 620 km in diam, represents a close approximation of the original crater rim, and the inner Rook ring corresponds to a central peak ring.

(3) The *Cordillera Mountain scarp* (900 km diam), which defines the Orientale basin, formed during the latter phases of the Orientale cratering event as a mega-terrace downfaulted toward the crater interior.

(4) The *domical facies* originated during the downfaulting of the Cordillera scarp by seismic and slump modification of an originally radially textured ejecta blanket.

(5) The *corrugated and plains facies* are intimately interrelated and are confined to the crater interior. Based on their distribution and characteristics, they are interpreted to be mixtures of shock-melted material and partially melted to unmelted ejecta material, with the plains units being the least contaminated with unmelted material. Identification of the crater within the Orientale basin and its associated deposits allows estimates of areas of shock-melted material to be made. Shock melts and shock melt-clast mixtures cover an area about 255000 km^2 on the crater floor. The plains unit covers an area about 75000 km^2.

(6) Lack of major post-emplacement *structural deformation* of these interior deposits indicates that major structural readjustments associated with the formation of the Cordillera scarp were completed prior to the final cooling of these units.

(7) The *mare deposits* are relatively younger than the crater floor deposits and are very small in area (Mare Orientale, 50000 km^2; Veris, 12500 km^2; Autumni 5000 km^2) compared to other basin deposits and mare deposits in other basins. Veris and Autumni may be nearly contemporaneous with the basin formation.

(8) *Gravity* – The present study suggests that the Orientale basin configuration is very nearly the same as its geometry at its time of formation. In addition, the volume of mare fill is reasonably small compared to other mascon basins. Sjogren *et al.* (1972) have mapped a mascon associated with the Orientale basin. Since there is little evidence of subsequent structural modification of the crater or extensive mare fill, this implies that the Orientale mascon formed in relation to the cratering event, rather than at a later time. The striking geophysical implication of this (Head, 1974a) is that mascon formation for a major multi-ringed basin may be primarily related to crustal excavation and upwarping of a 'moho' plug, as suggested by Wise and Yates (1970), and that the super-isostatic configuration of most multi-ringed basins is not simply a function of post-impact mare filling.

(9) *Origin of plains* – The intermediate albedo plains on the floor of Orientale are shown to be related to impact melting and deposition during the cratering event. Other occurrences of plains units within multi-ringed basins (Wilhelms and McCauley, 1971), such as those in Imbrium near the Apollo 15 site, may share a similar origin. Thus, large expanses of Cayley-like plains units may have originated from impact melting. Many other areas of Cayley plains occur within smaller craters. The Cayley plains at the Apollo 16 site appear to lie on the floor of an old 60 km diam crater (Head, 1974d). Thus, the regionally flat plains units within multi-ringed basins and many highland craters may have been produced by ponding of impact-induced melts. Subsequent contributions were probably made to these original flat surfaces in older craters (Head, 1974b, d).

(10) *Magnetics* – If the impact-induced melts units observed in Orientale cooled in the presence of a magnetic field, they would presumably show distinct magnetic characteristics. Many of the magnetic anomalies detected on the lunar farside (Russell, *et al.*, 1973) which seem unrelated to local surface geology, may be major impact melt units obscured and partly buried by subsequent events.

6. Implications for Lunar Samples

The amount of melt produced by a given impact is primarily dependent on total impact energy and the partitioning of this energy, two factors which are not exactly known. Since the velocity and mass of the body which produced the crater are also unknown, several workers have attempted to devise a mathematical relationship be-

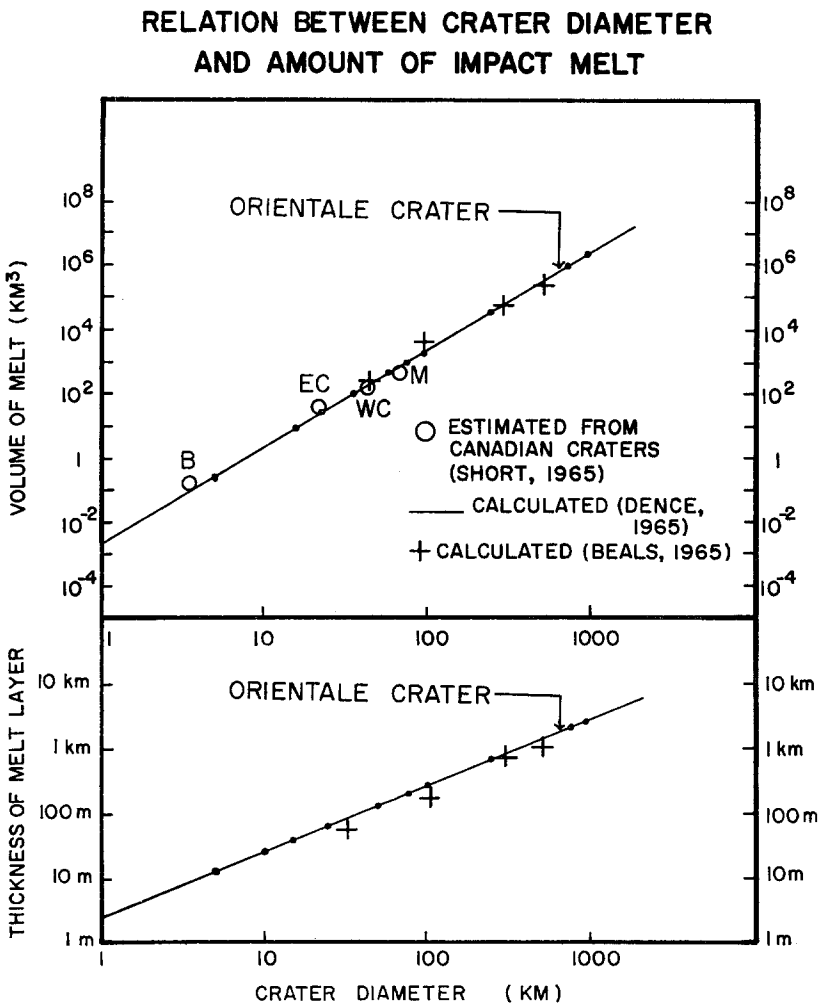

Fig. 17. Relations between crater diameter and amount of impact melt formed by direct fusion of target rock. The straight line is based on estimated melt volumes at known Canadian craters, using the relation, $V_{melt} = 0.002D^3$, where D is the crater diameter in km (Dence, 1965). Crosses are calculated from Baldwin's energy equations, assuming a 5% use of energy to melt rock (Beals, 1965). Large open circles are estimated melt volumes for several Canadian craters; *B*, Brent, Ontario; *EC* and *WC*, East and West Clearwater Lakes, Quebec; *M*, Manicouagan, Quebec (Short, 1965). Modified from French, 1970. Predicted volumes for Orientale crater are indicated.

tween the diameter of a crater and the energy of the impacting body. Most calculations are based on nuclear and chemical explosions scaled to larger crater diameter, but uncertainties in the extrapolations in energy and diameter for large meteorite craters are so great that calculated energies for specific diameters may vary by one or two orders of magnitude (French, 1970). Energy partitioning is also not well understood. Gault and Heitowit (1963) have estimated that about 20% of the impact energy in small-scale hypervelocity impacts is transmitted to the target as thermal energy. The proportion of this energy which is dissipated, as opposed to melting the target rock, is not known (French, 1970).

Dence (1965) and Short (1965) have estimated melt volumes from detailed studies of several Canadian craters and Beals (1965) has calculated melt volumes which are in close agreement with these observations and estimates. A summary of calculated melt volumes and melt thicknesses (assuming 5% of the impact energy is used to melt the rock) is presented in Figure 17 (French, 1970).

As previously mentioned, impact melted rock occurs in two major modes in terrestrial impact craters: (1) as glassy fragments and crystalline matrix in breccias, and (2) as discrete layers of melted rock which are completely recrystallized and resemble igneous rocks. The characteristics of these discrete melt layers include (Dence, 1968; French, 1970): (1) chemical composition similar to that of the underlying target rock, (2) absence of phenocrysts, (3) absence of flow structure, indicating crystallization virtually in place, (4) generally fine grain size with quench textures in glassy varieties, (5) association with distinctly shocked and shock-melted breccias.

6.1. Orientale basin

Using the relations between crater diameter and amount of impact melt shown in Figure 17, one would predict that Orientale (620 km diam) might have produced 200000–300000 km^3 of impact melt and a possible melt layer at least a kilometer thick. The estimated total area in Orientale covered by the corrugated and plains facies is about 255000 km^2 (accepting the evidence that these facies underlie the maria). The plains facies are interpreted to be the most intensely shock melted portion of the floor because of their smooth surface, their occurrence in ponded lows, their crack distribution and width, and their occurrence toward the crater center, similar to the position of terrestrial shock melt layers. The area covered by plains facies in the Orientale crater interior is estimated to be about 75000 km^2. Thickness of the plains facies is difficult to estimate, but if the cracks on the floor represent cooling and contraction of the shock melt layer, as they appear to, then their several hundred meter elevation suggests that the plains in the crater interior may be at least a kilometer in thickness. Thickness of the corrugated facies are certainly variable, but based on its draped appearance and relation to underlying topography, it probably averages at least a kilometer in thickness. To conclude the approximation, then, it appears that within the Orientale crater there is at least 75000 km^3 of intensely shock-melted material concentrated in the crater interior (plains facies) and at least 180000 km^3 of a mixture of shock-melted material and an undetermined percentage of breccia clasts

and fragments (corrugated facies). This agrees well with the prediction shown in Figure 17. Larger basins generate considerably larger melt volumes. The Imbrium crater (970 km in diam) would produce a volume of melt over 1 000 000 km^3.

6.2. Implications for the Genesis of Apollo Highland Rocks

Shock melting processes have been shown to be significant locally on the Moon, in particular at the Apollo 16 site (Head, 1974d; Warner *et al.*, 1973). The volumes of shock-melted material deposited as standing bodies on the floor of Orientale, however, represent a major source of highland igneous rocks and represent a lunar crustal process of major, if not dominant, significance for igneous petrogenesis. DeHon (1974) has estimated that the Mare Tranquillitatis lava fill, which was emplaced in an entirely different mode (as a series of lava flows) has a volume of about 252 000 km^3. The Columbia River plateau basalts are estimated to have a volume of about 200 000 km^3 (Waters, 1955, 1961; Kuno, 1969), and were extruded as a series of flows over several million years. The Orientale event shock-melted volumes of lunar crustal rocks comparable to those emplaced in Mare Tranquillitatis and the Columbia River plateau. The Orientale event also deposited this shock-melted material simultaneously with the formation of the crater rather than over a period of millions of years. Thus, the formation of multi-ringed basins such as Orientale provides a mechanism of instantaneously producing tremendous volumes of melted lunar crustal material. The characteristics of the corrugated facies suggest that this unit represents great volumes of impact partial melts while the characteristics of the plains suggest vast amounts of material which has probably undergone complete impact melting. The portion of the material concentrated on the floor of the crater in almost pure melt form has a thickness probably exceeding a kilometer. Therefore, in addition to being produced instantaneously, the event forms a single igneous cooling unit of incredible proportions. Not only is this significant in terms of volume of melt produced, but it is also important in that the melt is produced and emplaced in such a way that extensive fractionation is possible. Cooling times associated with such thicknesses and volumes should be considerably longer than for thin flows. Textures and grain sizes associated with rocks formed from surface melts might mimic those found in igneous rocks formed at greater depths. The large surface areas also offer an opportunity for loss of any existing volatiles.

It is possible to generate a spectrum of highland igneous rock types from partial to total melting of a variety of highland crustal samples collected on lunar missions (Walker *et al.*, 1972; 1973a, b; Warner *et al.*, 1974). In addition, textural and compositional evidence from highland samples suggests that impact induced fractionation is an important process (Warner *et al.*, 1974). The mineralogy, textures, and crystallization histories of highland igneous rocks seem quite compatible with an impact melt origin. Therefore, the role of impact melting induced by large cratering events such as Orientale should be seriously considered in highland igneous petrogenetic models.

In summary, multi-ringed basin formation provides a mechanism for instantaneously melting large volumes of shallow to intermediate depth lunar crustal material and

emplacing it in such a way as to allow for the differentiation and crystallization of a variety of igneous rock types and textures.

Acknowledgments

This study grew out of discussions with Apollo 15 Commander David R. Scott. His excellent observations on the lunar surface and from lunar orbit raised many questions about lunar multi-ringed basins and their deposits. This study attempts to address several of these questions.

This work was performed under National Aeronautics and Space Administration grant NGR-40-002-116, which is gratefully acknowledged. Thanks are extended to the National Space Science Data Center for providing many of the photographs used in this study and to Ewen Whitaker of the Lunar and Planetary Lab for providing the Earth-based photography. Observations of the limb regions were undertaken using the 12″ refractor at Brown University's Ladd Observatory. Mr Dan Dickinson provided considerable help in early stages of this study through mapping and photogeologic analysis. The help of Ross Stein, Margie Power, Sally Bosworth, and Margaret Cummings in discussion and preparation of the manuscript is gratefully acknowledged.

References

Baldwin, R. B.: 1963, *The Measure of the Moon*, University of Chicago Press, Chicago, 488 pp.
Baldwin, R. B.: 1969, *Icarus* **11**, 320–331.
Baldwin, R. B.: 1972, *Phys. Earth Planetary Int.* **6**, 327–339.
Baldwin, R. B.: 1974, 'On the Origin of the Mare Basins', *Lunar Science V*, The Lunar Sci, Inst. p. 31.
Beals, C. S.: 1965, *Ann. N.Y. Acad. Sci.* **123**, 904–914.
DeHon, R. A.: 1974, 'Thickness of Mare Material in the Tranquillitatis and Nectaris Basins', *Lunar Science V*, The Lunar Sci. Inst. p. 163–164.
Dence, M. R.: 1964, *Meteoritics* **2**, 249–270.
Dence, M. R.: 1965, *Ann. N.Y. Acad. Sci.* **123**, 941–969.
Dence, M. R.: 1968, in B. M. French and N. M. Short (eds.), *Shock Metamorphism of Natural Materials*, p. 169–183, Mono Book Corp., Baltimore, 644 p.
Dence, M. R.: 1971, *J. Geophys. Res.* **76**, 5552–5565.
Engelhardt, W. von: 1972, 'Impact structures in Europe', *International Geological Congress*, Section 15 (Planetology), Montreal, Canada, p. 90–111.
French, B. M.: 1970, *Bull. Volcanol.* (2) **34**, 466–517.
Gault, D. E. and Heitowit, E. D.: 1963, *Proc. Sixth Hypervelocity Impact Sympos.* **2**, 419–526.
Green, J. and Short, N. M.: 1971, 'Volcanic Landforms and Surface Features', *A Photographic Atlas and Glossary*, Springer-Verlag, New York, 519 p.
Hartmann, W. K.: 1964, *Comm. Lunar Planetary Lab.* **2**, no. 36, 175–191.
Hartmann, W. K.: 1972, *Icarus* **17**, 707–713.
Hartmann, W. K. and Kuiper, G. P.: 1962, *Comm. Lunar Planetary Lab.* **1**, 51–66.
Hartmann, W. K. and Wood, C. A.: 1971, *The Moon* **3**, 3–78.
Hartmann, W. K. and Yale, F. G.: 1968, *Comm. Lunar Planetary Lab.* **7**, 131–137.
Hartmann, W. K. and Yale, F. G.: 1969, *Sky Telescope* **37**, 1–4.
Head, J. W.: 1973a, 'Origin of Morphologic Components of the Hevelius Formation', Lunar Orientale basin (Abs), *Geol. Soc. Am.*, 1973 Ann. Mtg., p. 661.
Head, J. W.: 1973b, *EOS* **54**, 1126–1127.
Head, J. W.: 1974a, 'Some Geologic Observations Concerning Lunar Geophysical Models', *Proceedings of the USSR-US Conference on the Cosmochemistry of the Moon and Planets*, in press.

Head, J. W.: 1974b, 'Processes of Lunar Crater Degradation: Changes in Style with Geologic Time', submitted to *Icarus*.
Head, J. W.: 1974c, *The Moon* **9**, 355–395.
Head, J. W.: 1974d, *The Moon* **11**, 77.
Kuno, H.: 1969, *Am. Geophys. Union, Am. Geophys. Monthly Ser.* **13**, 495–501.
McCauley, J. F.: 1964a, 'The Stratigraphy of the Mare Orientale Region of the Moon', U.S. Geol. Surv. Astrogeologic Studies Ann. Prog. Rept., August 1962–July 1963, Pt. A, p. 86–100.
McCauley, J. F.: 1964b, 'A Preliminary Report on the Geology of the Hevelius Quadrangle', U.S. Geol. Surv. Astrogeologic Studies Ann. Prog. Rept., August 1962–July 1963, pt. A, p. 74–85.
McCauley, J. F.: 1967a, 'Geologic Map of the Hevelius Region of the Moon', U.S. Geol. Survey Misc. Geol. Inv. Map I-491.
McCauley, J. F.: 1967b, in S. K. Runcorn, (ed.), *Mantles of the Earth and Terrestrial Planets*, p. 431–460.
McCauley, J. F.: 1968a, *Am. Inst. Aeron. Astron. J.* **6**, 1991–1996.
McCauley, J. F.: 1968b, in R. S. Saunders (ed.), *Problems for Geologic Investigations of the Orientale Region of the Moon*, and in G. E. Ulrich (ed.), *Advanced Systems Traverse Research Project Report*, U.S. Geol. Survey Interagency Report: Astrogeology 7, 59 p.
Oriti, R. A. and Green, J.: 1967, *Griffith Observer* **31**, 118–125.
Ridpath, I. and Murray, J.: 1970, *J. Brit. Astron. Ass.* **80**, 115–124.
Ross, C. S. and Smith, R. L.: 1960, 'Ash-Flow Tuffs: Their Origin, Geologic Relations, and Identification', U.S. Geol. Surv. Professional Paper, no. 366, 81 p.
Rükl, A.: 1972, *Astrophys. Space Sci. Library* **33**, 22 pp., 6 maps.
Russell, C. T., Coleman, P. J., Jr., Lichtenstein, B. R., Schubert, G., and Sharp, L. R.: 1973, *Proc. Fourth Lunar Sci. Conf.* **3**, 2833–2845.
Saunders, R. S.: 1968, in G. E. Ulrich (ed.), *Advanced Systems Traverse Research Project Report* U.S. Geol. Surv. Interagency Report: Astrogeology 7, 59 p.
Schaeffer, O. A. and Husain, L.: 1974, *Lunar Science V*, Lunar Sci. Inst., p. 663–665.
Scott, D. H.: 1974, *Geologic Map of the Orientale Region of the Moon*, U.S. Geological Survey, (in preparation).
Sheridan, M. F.: 1970, *Bull. Geol. Soc. Am.* **81**, 851–868.
Short, N. M.: 1965, *Ann. N.Y. Acad. Sci.* **123**, 573–616.
Short, N. M.: 1970, *Geol. Soc. Am. Bull.* **81**, 609–648.
Short, N. M. and Forman, M. L.: 1972, *Modern Geol.* **3**, 69.
Sjogren, W. L., Muller, P. M., and Wollenhaupt, W. R.: 1972, *Apollo 16 Preliminary Science Report*, NASA SP-315, p. 24-1–24-7.
Stuart-Alexander, D. and Howard, K.: 1970, *Icarus* **12**, 440.
Ulrich, G. E.: 1968, *Astrogeology* **7**, 59 p.
Van Dorn, W. G.: 1968, *Nature* **220**, 1102.
Van Dorn, W. G.: 1969, *Science* **165**, 693.
Walker, D., Longhi, J., and Hays, J. F.: 1972, *Proc. Third Lunar Sci. Conf.* **1**, 797–817.
Walker, D., Grove, T. L., Longhi, J., and Hays, J. F.: 1973a, *Earth Planetary Sci. Letters* **20**, 325–336.
Walker, D., Longhi, J., Grove, T. L., Stolper, E., and Hays, J. F.: 1973b, *Proc. Fourth Lunar Sci. Conf.*, 1013–1032.
Warner, J. L., Simonds, C. H., and Phinney, W. C.: 1973, *Proc. Fourth Lunar Sci. Conf.* **1**, 481–504.
Warner, J. L., Simonds, C. H., and Phinney, W. C.: 1974, *Lunar Science V*, The Lunar Sci. Inst., p. 823–825.
Waters, A. C.: 1955, *Geol. Soc. Am. Spec.* **62**, 703–722.
Waters, A. C.: 1961, *Am. J. Sci.* **259**, 583–611.
Wilhelms, D. E. and McCauley, J. F.: 1971, *Geologic Map of the Near Side of the Moon*, U.S. Geol. Survey, Misc. Geol. Inv. Map I-703.
Wise, D. V. and Yates, M. T.: 1970, *J. Geophys. Res.* **75**, 261–268.
Wood, C. A.: 1968, *Lunar Planetary Lab. Contrib.* **120**, 157–160.
Wood, C. A.: 1973, *Icarus* **20**, 503–506.